University of Groningen

Interaction of different cell types with magnesium modified by plasma electrolytic oxidation

Echeverry-Rendon, Monica; Echeverria, Felix; Harmsen, Martin C.

IMPORTANT NOTE: You are advised to consult the publisher's version (publisher's PDF) if you wish to cite from it. Please check the document version below.

Document Version
Publisher's PDF, also known as Version of record

Link to publication in University of Groningen/UMCG research database
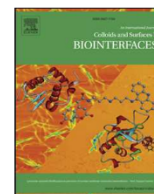
Interaction of different cell types with magnesium modified by plasma electrolytic oxidation

Monica Echeverry-Rendon[a,b,*], Felix Echeverria[a], Martin C. Harmsen[b]

[a] Centro de Investigación, Innovación y Desarrollo de Materiales CIDEMAT, Facultad de Ingeniería, Universidad de Antioquia UdeA, Calle 70 No. 52-21, Medellín, Colombia
[b] University of Groningen, University Medical Center Groningen, Department of Pathology and Medical Biology, Hanzeplein 1, EA11, NL-9713 GZ, Groningen, The Netherlands

ARTICLE INFO

ABSTRACT

Magnesium (Mg) is a material widely used in industrial applications due to its low weight, ductility, and excellent mechanical properties. For non-permanent implants, Mg is particularly well-suited because of its biodegradability, while its degradation products are not harmful. However, Mg is chemically reactive, and cytotoxic hydrogen gas is released as part of the degradation. This adverse degradation can be tuned using plasma electrolytic oxidation (PEO). With PEO, a surface layer of $MgO/Mg(OH)_2$ is deposited on the surface of Mg in a controlled way. The electrolytes used during PEO influence the surface's chemistry and topography and thus expectedly the biological response of adhered cells. In this study, thin samples of commercial pure of Mg (c.p Mg) were modified by PEO guided by different electrolytes, and the biological activity was assessed on vascular cells, immune cells, and repair cells (adipose tissue-derived stromal cells, ASCs). Vascular cells were more vulnerable than ASCs for compounds released by surface-coated Mg. All surface coatings supported the proliferation of adhered ASC. Released compounds from surface-coated Mg delayed but did not block *in vitro* wound closure of fibroblasts monolayers. Preformed endothelial tubes were vulnerable for released compounds, while their supporting ASC was not. We conclude that PEO-based surface-coating of Mg supports adhesion and future delivery of therapeutic vascular repair cells such as ASC, but that the observed vulnerability of vascular cells for coated Mg components warrants investigations *in vivo*.

1. Introduction

Cardiovascular disease (CVD) is a significant cause of morbidity and mortality globally and an increasing societal and public health burden [1]. The increased life expectancy, unfortunately, coincides with an increased risk for age-related CVD with is a global economic burden [2,3]. Nevertheless, CVD is a disease of the elderly only: risk factors such as a highly sessile lifestyle, emotional stress, smoking, high caloric nutrition, and obesity may set off CVD already before adulthood. Dysfunction of the intima of the may result in atherosclerotic lesions i.e., plaques. These plaques may progress and occlude the arterial lumen that obstructs blood flow and cause acute ischemia, such as myocardial infarction. Alternatively, atherosclerosis may progress to pathological widening via thinning of the arterial wall that is aneurysm development. Aneurysms with big sizes have an increased risk of rupture, which associates with more than fifty percent mortality [4,5]. Metal stents and coils have been used successfully to regain vascular integrity and architecture; however, this treatment may present long term complications such as vascular re-occlusion i.e., restenosis [6–9]. Throughout the history of the development of stents, different formulations have been evaluated that range from bare metal implants to drug-eluting stents and bioabsorbable vascular stents (BVAS) [10–12]. Nevertheless, the self-expanding bare metal stent still is most commonly applied. These consist of nickel-titanium alloys (Nitinol) or cobalt-chromium alloys and are permanent, undegradable implants. Implant failure is a continuing challenge e.g. unintentionally asymmetrically positioned stents to increase the risk for thrombosis. We argued that the 'next-generation' stent should have two main characteristics. Firstly, it should be biodegradable, while secondly, it should carry repair capacity that normalizes the arterial wall. Recently, a plethora of biodegradable stents has reached the marked, which performed similar to permanent (drug-eluting) metal stents [13]. These biodegradable stents are

---

Table 1
Coating obtained by plasma electrolytic oxidation on Mg samples.

Sample code	Composition of the electrolytic solution	Operation parameters
c.p Mg	Untreated	
NAF	$0.07\,M\ KOH + 0.1\,M\ Na_2SiO_3.9H_2O^* + 0.2\,M\ NaF$	$104.16\,mA\,cm^{-2}$, 600 s
HMT	$0.07\,M\ KOH + 0.1\,M\ Na_2SiO_3.9H_2O + 0.07\,M\ C_6H_{12}N_4^{**})$	320 V, 600 s
MAN	$0.07\,M\ KOH + 0.1\,M\ Na_2SiO_3.9H_2O + 0.05\,M\ C_6H_{14}O_6^{***}$	350 V, 600 s
NAF/HMT	$0.07\,M\ KOH + 0.1\,M\ Na_2SiO_3.9H_2O + 0.2\,M\ NaF\ /\ 0.07\,M\ KOH + 0.1\,M\ Na_2SiO_3.9H_2O + 0.07\,M\ C_6H_{12}N_4$	$104.16\,mA\,cm^{-2}$ 600 s/320 V, 600 s
NAF/MAN	$0.07\,M\ KOH + 0.1\,M\ Na_2SiO_3.9H_2O + 0.2\,M\ NaF/\ 0.07\ KOH + 0.1\,M\ Na_2SiO_3.9H_2O + 0.05\,M\ C_6H_{14}O_6$	$104.16\,mA\,cm^{-2}$ 600 s/350 V, 600 s

* Sodium metasilicate.
** Hexamethylenetetramine.
*** Mannitol.

composed of polymers or absorbable metals or their combination [14–17]. On average, these non-permanent stents are thicker than metal stents that make them protrude slightly above the implant site, which has been suggested to increase thrombosis risk.

In this study, we focus on Mg as a biodegradable metal for future stents. Mg is an essential element for the body because Mg^{2+} ions are co-factors of several enzymes; thus, many physiological processes depend on Mg [18,19]. Mg is even more abundant than sodium (Na) or potassium (K) in our body. One of the advantages of using Mg as a material is its high biocompatibility. Despite this, metallic Mg has some limitations to be used as an implant. In aqueous solution, Mg is highly reactive, and this reaction comprises the (fast) alkalization of the surrounding area by the formation of $Mg(OH)_2$. Additionally, during this oxidation of Mg, hydrogen gas is released. This gas may accumulate in the tissue and form highly cytotoxic gas pockets that inhibit wound healing and cause necrosis [20,21].

Alloys Mg with other metals improves the corrosion resistance and is applied in clinical stents meanwhile [22–24]. A different approach to increase corrosion resistance is to oxidize the surface of Mg and generate a protective oxide-based coating; this can be achieved with plasma electrolytic oxidation (PEO) which is a low cost, simple and effective technique which employs an electrochemical cell in which Mg is used as anode and oxidized in a controlled way [25]. By careful control of voltage, current density, time, and electrolyte solution composition, a protective layer of $MgO/Mg(OH)_2$ is grown on the surface. This layer is more chemically stable and thus decreases the rate of degradation of the underlying Mg [26–29]. We have previously optimized the conditions for surface modification of Mg by PEO by using organic additives in the electrolytic solution and changing the operation parameters such as voltage and current density. Finally, we obtained materials with different surface morphologies and also with better corrosion resistance. Once the material was characterized, it is necessary to study the biological performances of the material and the influence of the surfaces on different cell types present in a blood vessel [30].

Others showed that the accelerated degradation of Mg-based implants might cause a structural collapse, which is undesirable [31,32]. Material degradation demands to be synchronized to a normalization of the arterial wall; thus, structural collapses pose a challenge. The restoration of the arterial wall after stenting could likely be accelerated by the local administration of therapeutic cells such as adipose tissue-derived (mesenchymal) stromal cells (ASC). These are pro-angiogenic and may also differentiate to contractile medial smooth muscle cells [33,34]. Therefore, loading of ASC onto surface-coated Mg-stents might act as a double-edged sword: on the one hand, repair of the arterial wall is accelerated after balloon catheterization and stent placement. On the other hand, this will compensate for premature collapse to the integrity of Mg-based stents. Our study aimed to test the hypothesis that PEO-based surface-modified commercial pure magnesium (c.p Mg) loaded with regenerative cells, i.e., ASC, is a platform for arterial repair [35].

As a first (*in vitro*) approach, we investigated the response of different cell types and their function involved in the blood vessel context

after exposure to released degradation compounds, i.e., extracts, of uncoated c.p Mg and c.p Mg surface-coated by PEO.

2. Materials and methods

2.1. Materials and modifications

Chemically pure magnesium (c.p Mg) was processed into thin sections (10 × 10 × 1 mm), polished with a series of silicon carbide paper up to 1000 grade, cleaned with distilled water, sonicated in ethanol in an ultrasonic bath for 15 min and air-dried. Sections were surface-coated by plasma electrolytic oxidation (PEO) subsequently. Briefly, the thin sections were used as anode in an electrolytic cell connected to a power source where voltage, current density, and time were adjusted. PEO was performed as described previously for authors [30]; the specific conditions are listed in Table 1. Briefly, we used fluoride (NAF), hexamethylenetetramine (HMT), and mannitol (MAN) as additives for the electrolytic solution. The morphology, the structure, and the thickness of the coatings were studied after observation of the surfaces and cross-sections of the samples under scanning electron microscopy (SEM) (JEOL JSM 6940 L V). A complete characterization of the samples was described in detail on a previous study carried out for the authors [36]. Surface-coated Mg sections ('materials') and uncoated c.p Mg controls were stored at room temperature until use. Surface-coated materials and controls were used in cell culture experiments, and alternatively, materials were incubated in 1.2 mL culture medium (see below) for 48 h and the supernatant ('material's extracts') used in cell culture experiments.

2.2. Quantification of Mg^{2+}

Briefly, quantification of the Mg^{2+} concentration in the extracts from samples and control (culture medium) was done with the xylidyl blue-I method which is based on the reaction of Mg^{2+} ions with xylidyl blue reagent, sodium 1-azo-2-hydroxy-3-(2, 4-dimethylcarboxanilido)-naphthalene-1′-(2-hyd-roxybenzene-5-sulfonate) (Magnesium Gen.2, Roche Diagnostics, Netherlands) that yields a colored complex which is read by photospectrometry 505 nm and 600 nm.

Cell cultures were carried out with human skin fibroblasts (PK84), human smooth muscle cells (SMC), human adipose tissue-derived stromal cells (ASC), human monocytic (premyeloid) cell line THP-1 (ATCC, Virginia, USA) and human umbilical vein endothelial cells (HUVEC, Lonza, MD, USA). For their maintenance, PK84, hSMC, and ASC were cultured in DMEM (Lonza Biowhittaker, Verviers, Belgium) supplemented with non-inactivated 10% FBS, 1% penicillin/streptomycin (Gibco, Invitrogen, Carlsbad, CA) and 2 mM L-glutamine (Lonza, Biowhittaker, Verviers, Belgium). The THP-1 were maintained in RPMI-1640 (Biowhittaker, Verviers, Belgium), supplemented with 10% heat-inactivated FBS (Thermo Scientific, Hemel Hempstead, UK), 1% penicillin/streptomycin (Gibco, Invitrogen, Carlsbad, CA) and 2 mM L-glutamine (Lonza, Biowhittaker, Verviers, Belgium). Finally, HUVEC were cultured in flasks pre-coated with 0.1% gelatin, in endothelial culture

medium (ECM) consisting of RPMI-1640 (Biowhittaker, Verviers, Belgium), 10% heat-inactivated fetal bovine serum (FBS) (Thermo Scientific, Hemel Hempstead, UK), 0.06 mg/mL of home-made bovine brain-derived extract ('endothelial cell growth factor,' ECGF), 0.1 mg/mL heparin (Leo Pharma, Netherlands), 1% penicillin/streptomycin (Gibco, Invitrogen, Carlsbad, CA), 2 mM L-glutamine (Lonza, Biowhittaker, Verviers, Belgium). Cells were maintained at 37 °C, 5% CO^2, and 98% humidity.

2.3. Cell viability assay

The measurement of the mitochondrial activity determined the toxicity of the materials through the MTT assay. For this purpose, all cell types were cultured in 96 wells plates at a concentration of 50,000 cells/cm^2 until confluence. Next, the medium was removed and replaced with 100 μl of twofold serial dilutions of materials' extracts.

Cells were incubated at 37 °C, 5% CO_2, and 98% humidity for 48 h. Then, 20 μl per well of 3-(4,5-Dimethyl-2-thiazolyl)-2,5-diphenyl-2H-tetrazolium bromide) (MTT, Sigma-Aldrich, St. Louis, Missouri, USA) at 5 mg/mL was added per well. Cells were incubated for 3 h. After that, the medium was removed, and 100 μl of dimethyl sulfoxide (DMSO, Sigma-Aldrich, St. Louis, Missouri, USA) was added to dissolve the deposited crystals. Absorbance was measured at 570 nm wavelength in a spectrophotometer (Biorad). The conversion of MTT of treated cells was normalized to untreated (control) cells and plotted as a fraction (%) of mitochondrial activity (MTT is converted by mitochondrial succinate dehydrogenase). Measurements were performed in triplicate and repeated at least three times independently. Mean, and deviation standard was calculated and plotted using GraphPad-Prism7 (GraphPad, CA, USA).

2.4. Cell-material interaction

Surface-coated materials with dimensions of $10 \times 10 \times 1$ mm, and controls were seeded with 100 μL ASC at 100,000 per cm^2 in individual wells of 12 wells plates. After 30 min, 1 mL of medium was carefully added, and the cells were incubated at 37 °C for 48 h. Next, the medium was removed, and samples washed twice with PBS and fixed with 2% paraformaldehyde in PBS for 30 min. Cytoskeleton i.e., F-actin, was visualized by staining with Phalloidin-iFluor 647 Reagent – CytoPainter (1:500, Abcam, Cambridge, U.K) and counterstaining of nuclei with DAPI (1:5000, Sigma-Aldrich, D9542, St. Louis, Missouri, USA,). Fluoromicrographs were taken with a TissueFAXs scanning microscope (TissueGnostics GmbH, Vienna, Austria).

2.5. Western Blot analysis

Proliferation and apoptosis of cells cultured in contact with materials' extracts from surface-coated and control magnesium sections were investigated with Western blotting. Cells were lysed in RIPA buffer and the protein concentration determined. Proteins (20 μg/lane) were separated in SDS-PAGE Gradient Gels (4–20%) (BioRad, California, USA). Next, proteins were transferred onto a nitrocellulose membrane (BioRad, California, USA). The membrane was blocked with 5% non-fat milk for 2 h, followed by overnight incubation at 4 °C with primary antibody, respectively directed against PARP (1:500, Santa Cruz, sc-7150, California, USA), caspase 3 (1:100, Cell Signaling, 9665S, Danvers, Massachusetts, USA), PCNA (1:2000, Cell signaling, 2586S, Danvers, Massachusetts, USA) or β-actin (1:2000, Cell Signaling, 4967 L, Danvers, Massachusetts, USA). Following incubation with HRP-conjugated goat anti-mouse IgG (Dako, P0447, California, USA) and HRP-conjugated rabbit anti-goat IgG (Cell Signaling Technology, 7054S, Danvers, Massachusetts, USA) at room temperature for 2 h, proteins were visualized using alkaline phosphatase method.

2.6. Wound healing – scratch assay

For the wound-healing assay, the materials' extracts were used. In addition, conditioned medium (ASC-Cme) was collected from cultures of ASC (seeded at 100,000 per cm^2) on surface-coated materials and c.p Mg controls after 48 h. Sentinel cells used for the assay were PK84 fibroblasts seeded at 10,000 per cm^2 in 24 wells tissue plates and used upon reaching confluency. A straight scratch was made across the center of the well with a 200 μl pipette tip simulating a wound. Wells were washed with PBS to remove detached cells and fragments. Next, 0.5 mL of materials' extracts or 0.5 mL of ASC-Cme were added, and the cellular responses monitored for 24 h. Micrographs were taken every 8 h with a Leica DMRXA inverted microscope and processed with Leica Software of Leica Microsystems (Wetzlar, Germany). The relative wound size at each time point was analyzed using ImageJ 1.48v (Wayne Rasband National Institutes of Health, USA), values were normalized to the initial wound size. Experiments were performed in triplicate and done three times independently.

2.7. Cell differentiation of ASC

Initially, cells were treated with materials' extracts for 48 h. Then for osteogenic and myogenic differentiation capacity of confluent monolayers of ASC (passage 3–7) was initiated with a differentiation medium (see below) that was changed twice per week for two weeks. Then, cells were fixed, and their cell types assessed by staining. For adipogenic differentiation, ASC was treated with 0.1 μM of dexamethasone (Pharmacy UMCG, Netherlands), 1 nM of insulin (Gibco, 41400-045, Waltham, Massachusetts, USA), 0.05 mM 3-isobutyl-1-methylxanthine (IBMX) (Sigma-Aldrich I5879, St. Louis, Missouri, USA). Cells were stained with oil red solution. For osteoblastic differentiation, ASC was exposed to 0.1 μM of dexamethasone (Pharmacy UMCG), 10 mM of β-glycerophosphate (Sigma, G9891, Sigma-Aldrich, St. Louis, Missouri, USA), 0.05 mM ascorbic acid (Sigma, A4544, Sigma-Aldrich, St. Louis, Missouri, USA). Cells were stained with alizarin red. For adipogenic and osteogenic staining, cells were assessed with an inverted optical microscope Leica DMRXA microscope and Leica software. Finally, for smooth muscle differentiation, ASCs were treated with 5 ng/mL of Recombinant Human TGF-β1 (Peprotech, NJ, USA). After two weeks cells were fixed and stained with antibodies against SM22α (1:500, Abcam, ab14106, Cambridge, U.K), phalloidin (1:500, A12379, Thermo Fisher Scientific, Waltham, Massachusetts, USA), and DAPI (1:5000, Sigma-Aldrich, D9542, St. Louis, Missouri, USA). As a secondary antibody Alexa fluor 647 donkey anti-rabbit IgG H&L (Abcam, ab150075, Cambridge, U.K). Stained cells were recorded with a TissueFAXs microscope (TissueGnostics GmbH, Vienna, Austria).

2.8. Co-culture of ASC and HUVEC

To assess the influence of materials' extracts from surface-coated materials and c.p Mg, the vasculogenic capacity of HUVEC on ASC monolayers in wells of a 24 well plate was determined in two manners [37,38]. Firstly, ASCs were exposed to two materials' extracts for 24 h. Next, the medium was removed and a single cell suspension of HUVEC was seeded at 10,000 per cm^2. The formation of vascular networks was monitored for seven days. Secondly, HUVEC were seeded on top ASC monolayers at 10,000 per cm^2 and incubated for seven days to allow vascular networks to form. Next, the medium was replaced with materials' extracts and further incubated for 24 h. At the end of the experiment, for both types of treatment, cells were washed twice and fixed with 2% paraformaldehyde in PBS for 30 min. Cells were permeabilized with 0.5% Triton X-100 (Sigma-Aldrich, St. Louis, Missouri, USA) for 15 min. Next, cells were incubated with monoclonal mouse anti-human CD31 (1:100, Dako, Clone JC70A, California, USA) for the detection of endothelial cells and rabbit polyclonal SM22α (1:100, Abcam, ab14106, Cambridge, U.K) for 2 h. Then cells were washed with

Table 2
Primer sequence for RT-qPCR.

Gene	Protein	Forward	Reverse
TNFA	Tumor Necrosis Factor Alpha	CAGCCTCTTCTCCTTCCTGAT	GCCAGAGGGCTGATTAGAGA
CCL2	Monocyte Chemotactic Protein 1	AGTCTCTGCCGCCCTTCT	GTGACTGGGGCATTGATTG
IL6	Interleukin-6	AGCTCAATAAGAAGGGGCCTA	TGAGAAACCCTGGCTTAAGTAGA
IL8	Interleukin-8	CTTTCAGAGACAGCAGAGCA	ACACAGAGCTGCAGAAATCA
IL1B	Interleukin-1beta	AAGCTGGAATTTGAGTCTGC	ACACAAATTGCATGGTGAAG
FGF2	Fibroblast growth factor-2	CTGTACCCATACAGCAGCAG	CGCCTAAAGCCATATTCATT
IGF1	Insulin-like growth factor-1	ACTCGGGCTGTTTGTTTTAC	GTGTGCTTCTTGACGACTTG
HGF	Hepatocyte growth factor	GTTTCCCAGCTGGTATATGG	GGTCTTTTCAGGAATTGTGC
COL4A1	Collagen type-IV alpha-1 chain	CAGCAACGAACCCTAGAAAT	CAATGAAGCAGGGTGTGTTA
FN1	Fibronectin	TCAACTCACAGCTTCTCCAA	TTGATCCCAAACCAAATCTT
VEGFA	Vascular endothelial growth factor-A	CCTGAAATGAAGGAAGAGGA	AAATAAAATGGCGAATCCAA
ANGPT2	Angiopoietin-2	CAGTTCTTCAGAAGCAGC	TTCAGCACAGTCTCTGAA
GAPDH	Glyceraldyde-3-phospate dehydrogenase	AGCCACATCGCTCAGACAC	GCCCAATACGACCAAATCC

PBS and incubated with secondary antibodies Alexa Fluor 488 Donkey anti-Mouse IgG (H + L) (1:300, Life technologies, A-21202, California, USA) and Alexa Fluor 647 Donkey anti-Rabbit IgG (H + L) (1:300, Life technologies, A31573, California, USA) for 1 h. Samples were preserved in PBS and images recorded using a TissueFAXs microscope (TissueGnostics GmbH, Vienna, Austria).

2.9. RNA isolation and RT-qPCR

ASCs from three different donors were cultured in $25\,cm^2$ tissue culture flasks until reaching confluence and treated with material's extracts. After that, RNA was extracted with TRIzol reagent (Invitrogen Corp, CA, USA) according to the manufacturer's protocol. RNA was obtained of each sample, and 5 ng of cDNA was amplified in 384-well microtiter plate in a TaqMAN ABI7900HT cycler (Applied Biosystem, Foster, California, USA) in 5 μl of SyberGreen universal PCR Master Mix (BioRad, California, USA) and 0.5 μl of 6 μM primer mix containing forward and reverse components. Amplimers of interest were detected by using the primer set reported in Table 2. The results of each conditioned medium are presented as fold changes in gene expression to their respective experimental controls.

3. Results

3.1. Surface characterization of the anodic coatings

SEM images show porous surfaces produced by the continuous melting–oxidation of the material representative of the PEO process (Fig. 1). The pore size for the NAF samples was about 0.4 μm, which was lower in comparison with the rest of the samples that were about 1.3 μm. The cross-section showed that all the coatings consisted of a network of interconnected porous. The thicknesses of the coatings were in the range between 3 and 5 μm. In all the coatings, a dense barrier layer isolating the coating to the substrate was observed (Fig. 1).

3.2. Surface-coating reduced release of Mg^{2+} into the culture medium

On average, surface-coated materials, irrespective of the electrolytes used during PEO, released an additional ~$3.2\,mM\ Mg^{2+}$ into the culture medium, which itself contained approximately $0.7\,mM\ Mg^{2+}$ (Table 3). The type of surface-coating did not influence the release of Mg^{2+} into the medium. However, the release from c.p Mg controls was almost twofold higher compared to surface-coated Mg i.e., $6.7\,mM\ Mg^{2+}$ (Table 3).

3.3. Extracts from materials show a cell type-dependent cytotoxicity

Undiluted extracts from all materials, irrespective of the type of coating, were cytotoxic for both vascular cell types that were assessed

i.e., endothelial cells (HUVEC) and vascular smooth muscle cells (SMC), albeit to a different extent (Fig. 2). Monocytic, macrophage-like cells (THP-1), ASC, and fibroblasts (PK84) were refractory to the cytotoxic influence of extracts at any of the tested concentrations. Controls, extracts from c.p Mg, were highly cytotoxic to all cell types tested. However, even two-fold diluted extracts from surface-coated materials were only minimally cytotoxic because all cell types had more than 70% viability (Fig. 2). Only incubation of HUVEC with extracts from MAN-modified material yielded a calculable IC50 (Mg concentration, which causes 50% cytotoxicity) of $13\,mM\ Mg^{2+}$. In contrast, c.p Mg extracts had IC50 values of $2.3\,mM\ Mg^{2+}$ for HUVEC. For SMC, ASC, THP-1, and PK84, IC50 values were not possible to calculate because the curves descended over one dilution step i.e., these extracts were non-cytotoxic.

3.4. The surface coating improves ASC adhesion

Twenty-four hours after seeding on resp. NAF, HMT, and MAN surface-coated materials, ASC had adhered and formed an almost confluent monolayer similar to their adhesion on tissue culture plastic (Fig. 3). A similar adhesion was observed for ASC on resp. NAF-HMT and NAF-MAN-coated materials.

In contrast, c.p Mg poorly supported adhesion of ASC: only a few blebbed cell remnants and ditto nuclei were observed, indicative of apoptosis. Interestingly, ASC on NAF-modified surfaces was elongated and spindle-shaped and aligned to the topography of the surface, which was left behind after polishing with sandpaper. On the other surface-coated surfaces, ASC had arranged randomly and had a typically mesenchymal appearance with two or more protrusions that were suggestive of these migrating on the surface (Fig. 3).

3.5. Surface coating of materials does not affect the proliferation or apoptosis of adhered ASC

The formation of monolayers on surface-coated Mg suggested the cells had proliferated and that apoptosis was suppressed. Immunoblotting analyses of ASC adhered to surface-coated materials revealed similar expression of the proliferation marker PCNA compared to ASC on tissue culture plastic (Fig. 4) irrespective of the type of coating. Non-coated c. p Mg surfaces could not be analyzed due to the virtual absence of cells, as described in the previous section. Treatment with puromycin reduced proliferation i.e., PCNA expression. Puromycin induced apoptosis in ASC from all three donors. In contrast, apoptosis of ASC adhered to surface-coated materials, irrespective of the type of coating, was comparable to plastic-cultured ASC both in terms of caspase-3 cleavage and PARP cleavage (Fig. 4). Only the controls (puromycin) showed markable cleavage of both caspase-3 and PARP i.e., confirmed apoptosis of ASCs.
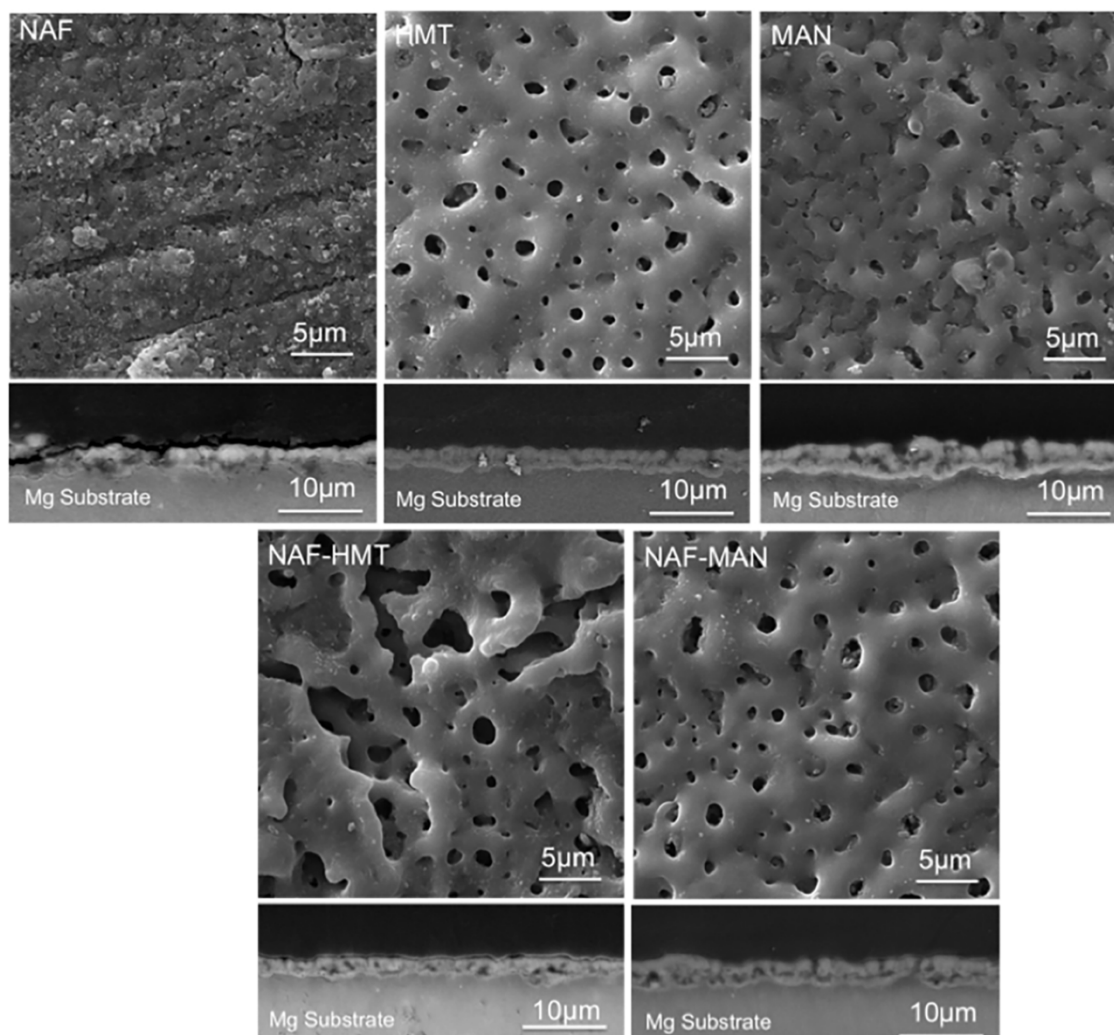
Fig. 1. Morphology of the coating after PEO process. SEM images shown the homogeneous topography if the coatings consisted of a network of interconnected porous. Cross-sections show the presence of a dense barrier layer between the coatings and substrate.

Table 3
Concentration of Mg^{2+} released from coated and uncoated samples of Mg.

Sample	Concentration Mg^{2+} (mM)
Control (culture medium)	0.68 ± 0.05
c.p Mg	7.38 ± 0.08
NAF	3.95 ± 0.01
HMT	3.89 ± 0.05
MAN	3.96 ± 0.01
NAF-HMT	3.92 ± 0.07
NAF-MAN	3.95 ± 0.01

3.6. Scratch wound healing is affected in a surface-coating-dependent fashion

Scratch wound healing *in vitro* of PK84 fibroblasts monolayers throughout 48 h was used to assess the influence of materials' extracts and conditioned medium from ASC (ASC-Cme) cultured on surface-coated materials. Untreated controls reached total wound closure between 24 h and 48 h irrespective of the presence of ASC-Cme (Fig. 5, suppl. Fig. 1). In contrast, l extracts from c.p Mg abolished wound closure (Fig. 5), even in the presence of ASC-Cme, while at 48 h cells had started to detach. In the presence of extracts from surface-coated materials, the wound closure followed first-order kinetics, which reached a plateau between 24 h and 48 h. The maximum levels of wound closure varied between 20%–70% of the controls in the absence of ASC-Cme, while ASC-Cme tended to reduce the maximum closure to between 10% and 50% (Fig. 5, representative micrographs in suppl. Fig. 1). The maximum level of wound closure appeared to be an experimental limitation. Therefore the rates of increase were determined, i.e., the slope of the curves. The summary of this behavior is shown in Table 4.

3.7. The differentiation capacity of ASC is not affected by surface-coated materials' extracts

Extracts from c.p Mg completely abolished the differentiation capacity of ASC to SMC, adipocytes, and osteoblasts, while in the absence of extracts, differentiation had occurred to these three lineages in the cell type-specific differentiation media (Fig. 6). Qualitatively, extracts from resp. NAF, MAN, HMT, NAF-MAN, and NAF-HMT surface-coated materials did not influence differentiation to SMC, adipocytes, and osteoblasts compared to controls (Fig. 6). Briefly, SMC differentiation generated SM22α -expressing spindle-shaped cells. Adipocytic differentiation was of low efficiency in the ASC donors that were assessed but presented as Oil-Red-O revealed lipid-filled cytoplasmatic vacuoles. Similarly, osteogenic differentiation was low under all conditions, including controls, but Alizarin-red, calcium phosphate, deposits were clearly distinguishable in all conditions except c.p Mg extracts and undifferentiated controls.
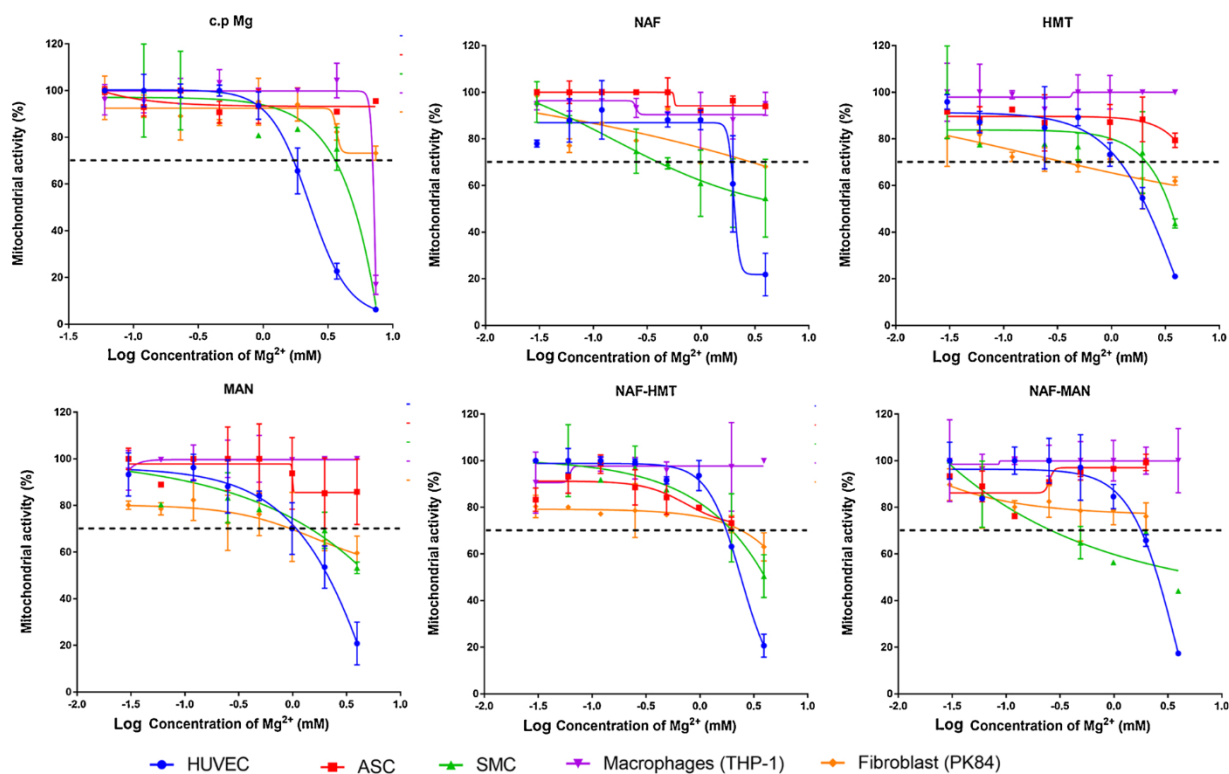
Fig. 2. Toxicity of different cell types after exposure to extracts. The response of ASC (red), HUVEC (blue), SMC (green), PK84 fibroblasts (orange) and THP-1 monocytes/macrophages (purple) to extracts of c.p Mg, and Mg coated with respectively NAF, HMT, MAN, NAF-HMT or NAF-MAN. Cytotoxicity was determined as mitochondrial conversion of MTT and plotted as fraction of control *i.e.* untreated cells against the magnesium concentration in the extracts. Data are the mean plus SD of n = 3 independent experiments with triplicate technical replicates.

3.8. In vitro, ASC-driven vasculogenesis is not affected in extracts -pretreated ASC, while extracts compromise performed vascular networks

Another functional assay was the evaluation of the synergistic interaction between ASC and HUVEC to promote the formation of new networks of blood vessels (vasculogenesis or vascular network formation, VNF) [36,37]. Through this experiment, more than the vitality, the functionality of both cell types was evaluated. In non-exposed controls, ASC (Fig. 7.B, red) promoted VNF by HUVEC (Fig. 7.B, green). The HUVEC arranged as tube-like structures that were surrounded by ASC. The pre-exposure of ASC to extracts did not influence their capacity to support VNF by HUVEC, except for c.p Mg extracts that abolished VNF.

The influence of extracts on already established vascular networks by ASC – HUVEC co-cultures was, however, vulnerable to exposure to extracts. The morphological integrity of control vascular networks remained intact over the entire period of the experiment (Fig. 7.C). The exposure of pre-established vascular networks to c.p Mg extracts completely obliterated their integrity; only cellular debris was visible at the end of the experiment. The exposure of pre-established vascular networks to extracts from surface-coated materials compromised the integrity of the endothelial tubes (Fig. 7.C, green) while the ASCs' integrity (Fig. 7.C, red) appeared to be unaffected. The HUVEC that comprised the tubes had lost intercellular connections and had a rounded appearance suggestive of apoptosis. The ASC retained their typical mesenchymal, fibroblast appearance and showed no morphological signs of apoptosis. This would appear to confirm our earlier observations that endothelial cells are vulnerable to l extracts while ASCs are not.

3.9. Extracts from surface-coated materials do not negatively affect the expression of therapeutic genes in ASC

In controls ASCs cultured on plastic, expression of inflammatory genes compared to GAPDH was low for TNFA, IL1B and IL8, and moderate for IL6 and CCL2 as expected. In controls, of the pro-angiogenic genes, VEGFA was highest expressed and ANG2 virtually not while related growth factor genes, FGF2, HGF, and IFG1, were moderately expressed. In contrast, both two genes that represent extracellular matrix, COL4A1, and FN1 were highest expressed of all genes studied. The treatment of ASCs with extracts from c.p Mg or surface-modified materials did not cause significant changes in gene expression on average. In general, changes in expression of all genes were within one log scale i.e., less than tenfold. Also, if any, tendencies in change of gene expression were either towards upregulation or downregulation, but not both. The resilience of ASCs to extracts from c.p Mg appeared to be reflected in their gene expression profile because none of the inflammatory genes were upregulated, while pro-angiogenic and matrix genes also remained similarly expressed (Fig. 8). The expression of CCL2, encoding the chemoattracting CCL2 (MCP-1), was, however, upregulated strongly in ASCs treated with extracts from HMT, NAF-HMT, or NAF-MAN surface coated materials. The expression of HGF was more variable than the other genes because it tended to increase by NAF extracts while HMT and NAF-MAN extracts reduced its expression. Thus, extracts had virtually no influence on the expression of genes representative of inflammation, angiogenesis, and extracellular matrix with few exceptions.

4. Discussion

In a past study, authors found the c.p Mg coated by PEO using HMT and MAN in the electrolytic solution, improves the corrosion resistance of the material and its biological performance. Considering an orthopedic application, that study showed that the produced coatings acts a protective layer to control the release of Mg without affecting the osteoblast viability and preventing thrombogenic effect [36]. With the purpose to explore another application, this study aimed to develop and
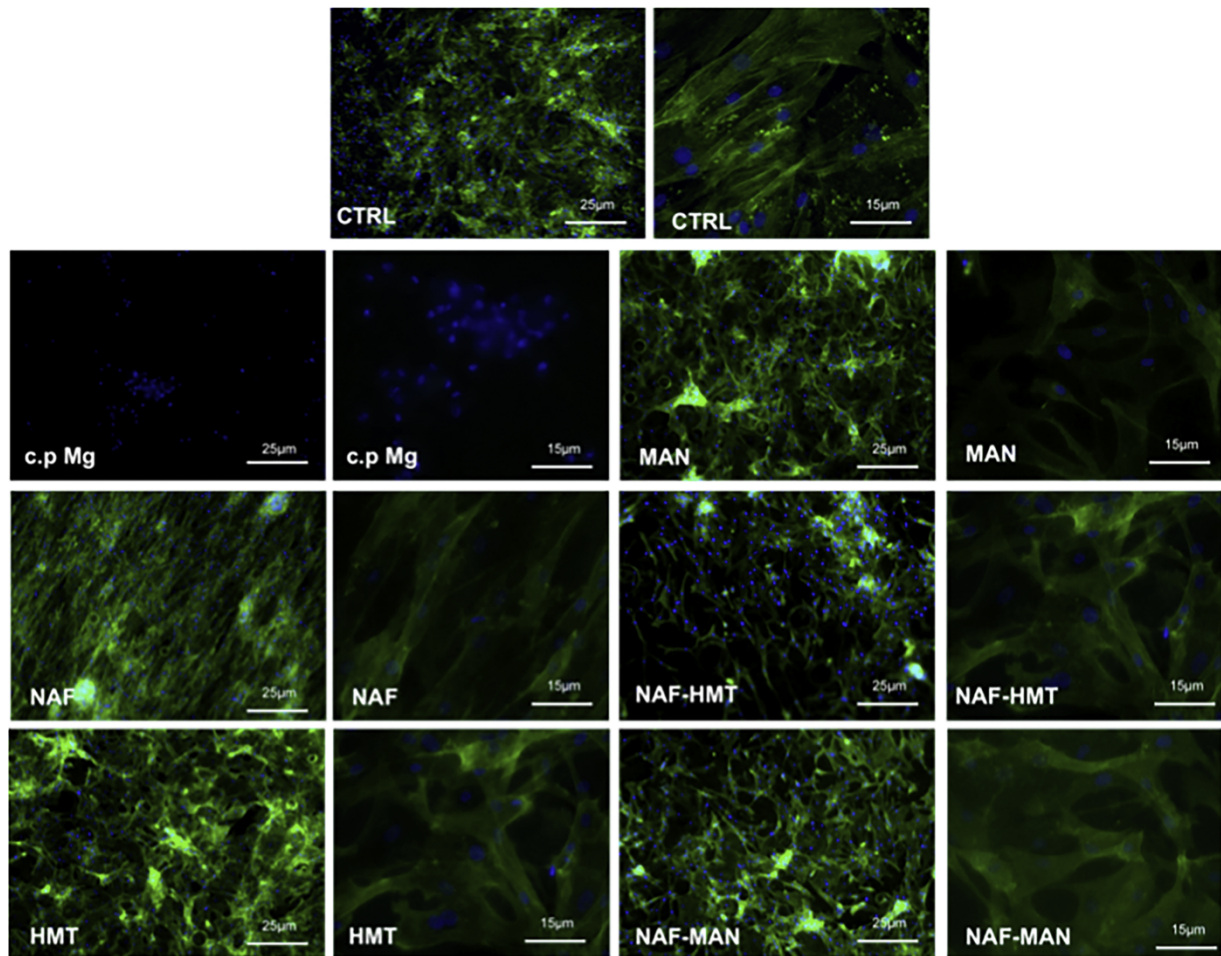
Fig. 3. ASC on surface-coated materials and controls. After 24 h of adhesion and proliferation on resp. tissue culture plastic (CTRL), c.p Mg, NAF, HMT, MAN, NAF-HMT and NAF-MAN-modified surfaces, cytoskeleton was visualized with phalloidin-FITC (green) and nuclei with DAPI (blue).

evaluate a temporary scaffold based on degradable anodized c.p Mg loaded with regenerative cells i.e., ASC for future use in stenting of arterial lesions. The main findings of our study are that by PEO surface oxidation, the cytotoxic and bio-incompatible c.p Mg is converted into a biocompatible material that supports adhesion of therapeutically relevant ASC. At the same time, it does not negatively affect their gene expression profile. The variation of electrolyte solution additives i.e., sodium fluoride (NAF), hexamethylenetetramine (HMT), and mannitol (MAN) or their combination (NAF-HMT and NAF-MAN) was of little influence to cytotoxicity or *in vitro* biological processes. While mesenchymal cell types (fibroblasts, ASCs) and immune cells (THP-1 monocytes) were refractory to extracts from surface-coated materials, vascular cell types (ECs and SMCs) were more vulnerable to their cytotoxic components. This was corroborated by the adverse influence of extracts on pre-established vascular networks *in vitro* in which the endothelial tubes disintegrated while the ASC remained viable. This was further confirmed in scratch wound closing assays in which extracts only reduced, but not abolished, the closure rate of damaged fibroblast monolayers.

After the implantation of a cardiovascular stent, the body response begins with the binding of plasma proteins to the surface of the material. In this process, parameters as surface energy and wettability are crucial, especially for ASCs, which will be in direct contact with the implant. PEO changes the surface configuration of the material, transforming the Mg in hydrophobic to a hydrophilic surface, favoring the deposition of proteins at the moment of the implantation [36,39,40]. Additionally, the porous topography increases the surface area improving the attachment of the ASCs. This morphology can also be used

as a vehicle for the deposition of growth factors, drugs, or proteins [41,42].

In aqueous solutions, the adverse biocompatibility and high cytotoxicity of (metallic) Mg are caused by oxidation, i.e., the formation of $Mg(OH)_2$ (corrosion product) that dissolves and raises the pH beyond physiologically tolerable levels. Besides, the corrosion of Mg releases cytotoxic hydrogen gas (H_2). We corroborated the cytotoxicity of c.p Mg on all evaluated cell types. Therefore, modification of the surface of c.p Mg was warranted to improve its biocompatibility and reduce its cytotoxicity. Indeed, PEO treatment of c.p Mg reduced the release of cytotoxic components, yet vascular cell types were more vulnerable than mesenchymal cell types such as fibroblasts and ASC while monocytes (THP-1) that play an essential role in arterial wound healing were refractory too. Extracts from Mg-Zn-Ca alloys caused increased proliferation of ASC, while pure Mg extracts were non-cytotoxic to ASC [38], which is at least partially confirmed by our results. Differences in extraction, materials, and ASC likely explain their resilience to pure Mg extracts. The Mg^{2+} concentration in the extracts may have been higher than in the study of Yazdi [43]. In general, mesenchymal cell types such as human umbilical cord perivascular cells [44], osteoblasts (U2OS) [45] are refractory to Mg^{2+} and respond in a concentration-dependent fashion.

The degradation of Mg-based biomaterials involves the release of particulate fragments that require phagocytic clearance by macrophages. Indeed, phagocytic uptake of corrosion products released from Mg-2.1Nd-0.2Zn-0.5 Zr alloys [46], pure Mg particles [47], does not negatively affect primary human macrophages. Larger sized particles, however, reduce the vitality of J774 macrophages after phagocytosis
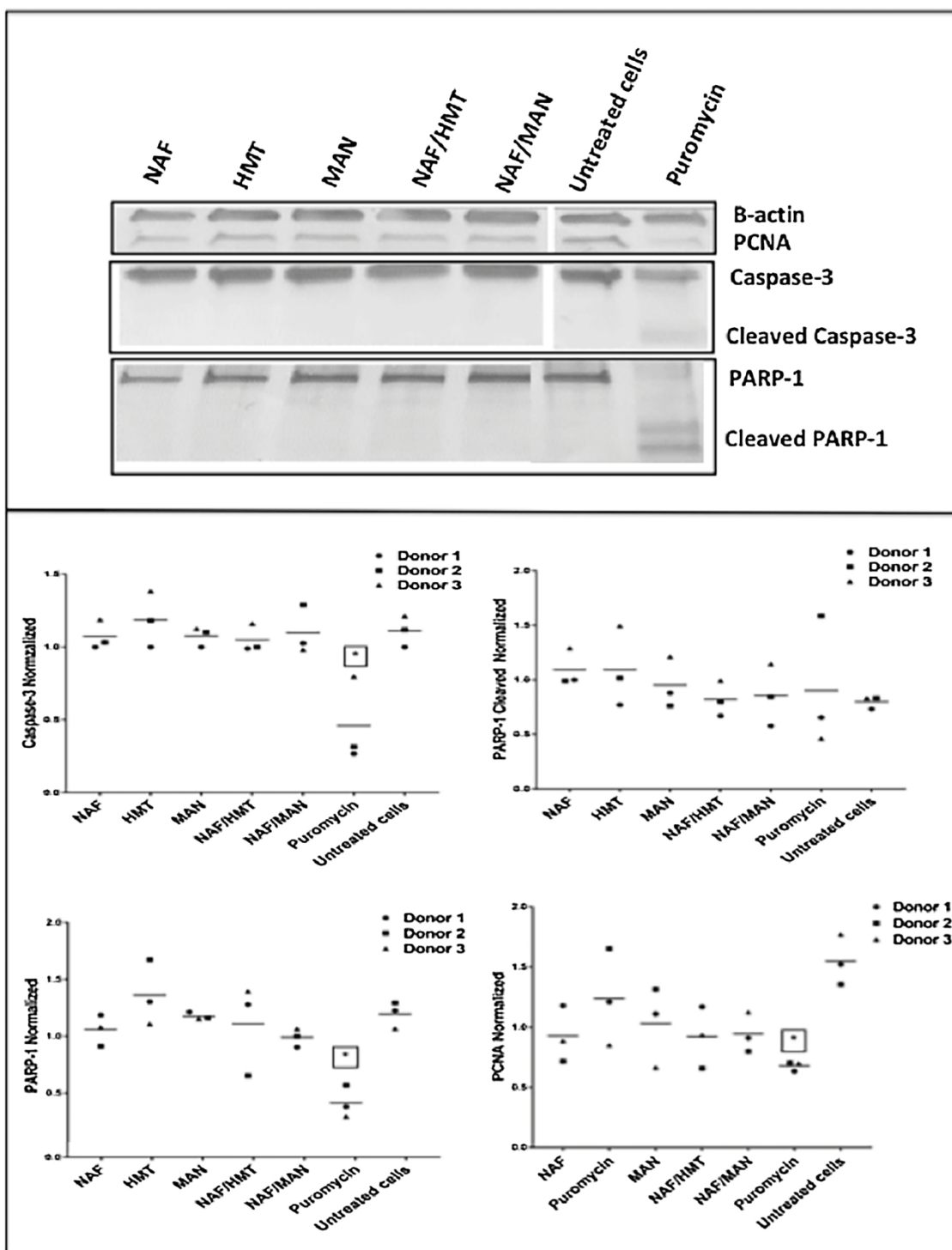
Fig. 4. Proliferation and apoptosis of ASC adhered to coated surfaces. Immunoblotting of cell lysates separated by SDS-PAGE with antibodies against PCNA (proliferation), caspase-3, which detects intact and cleaved caspase-3 (apoptosis) and PARP, which detects intact and cleaved PARP (apoptosis) ASCs were cultured materials coated respectively with NAF, HMT, MAN, NAF/HMT, NAF/MAN or tissue culture plastic. Untreated cells served as positive control for proliferation and negative control for apoptosis while puromycin treatment served as negative control for proliferation and positive control for apoptosis. All data were normalized with respect to β-tubulin. Data are the mean plus SD of n = 3 independent experiments with cells from three different donors.

[48]. Our results confirm that extracts released from surface-coated c.p. Mg did not induce a cytotoxic response in THP-1. Thus, while we did not assess the presence of nano and microparticulate fragments in extracts nor the Mg^{2+} concentration, the surface-coating is suitable to support the proper functioning of ASC and immune cells. As a matter of fact, surface-coated materials did not induce apoptosis i.e., cleavage of pro-caspase three nor PARP, in adhered ASC, while proliferation (PCNA expression) was maintained. The type of surface-coated had virtually no influence on the adhered ASC, although minor differences in cellular morphology were observed that cannot be explained based on the current data. In contrast, ASC adhered to the c.p Mg surface died by apoptosis, which emphasizes the protecting influence of either of our evaluated surface-coatings.

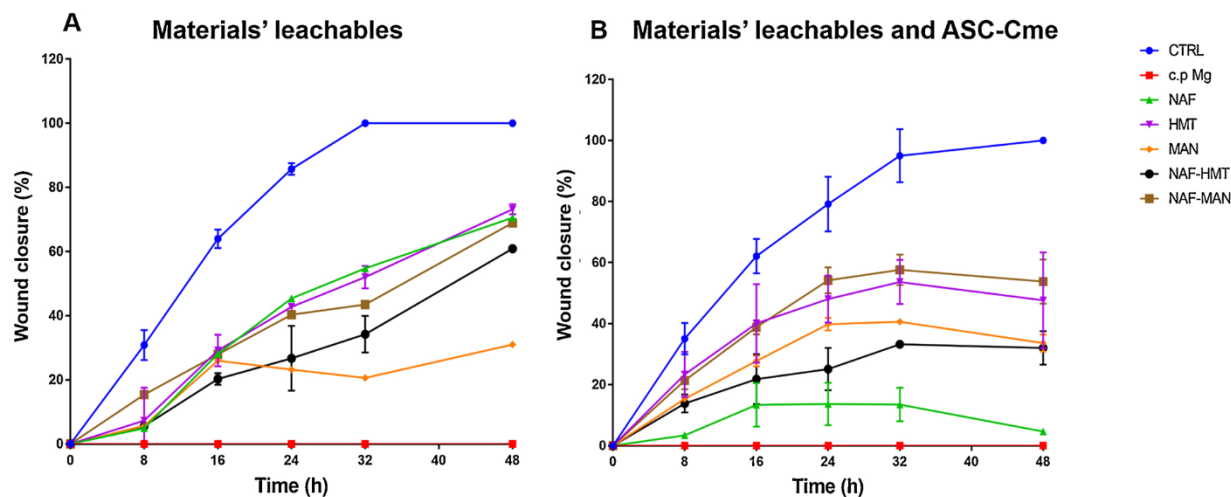The biological activity of ASC e.g., the capacity to support wound

Fig. 5. Scratch wound closure in PK84 fibroblast monolayers treated with materials' extracts and ASC-Cme. Confluent monolayers were scratched and wound healing monitored by microscopy during treatment with materials' extracts or with extracts supplemented with ASC-Cme. Materials' extracts were obtained by incubation in medium for 48 h from surfaces modified with DMEM (blue), DMEM + c.p Mg (red), DMEM + NAF (green), DMEM + HMT (purple), DMEM + MAN (orange), DMEM + NAF-MAN (black), DMEM + NAF-MAN (brown). Data are the mean plus SD of n = 3 independent experiments with triplicate technical replicates.

Table 4
Percentage of wound closure in the presence of extracts from surface-coated materials.

Surface coating	Material extracts (% / h)	Mat. extracts + ASC-Cme (% / h)	% Change
Control	3.1	3	n.a
c.p Mg	0	0	n.a.
NAF	1.7	0.8	↓0.9
HMT	1.6	2.0	↑0.4
MAN	0.6	1.3	↑0.7
NAF-HMT	1.1	1.0	n.a
NAF-MAN	1.4	1.9	↑0.5

closure or vasculogenesis and the secretion of beneficial paracrine factors and the absence of pro-inflammatory activation, was not affected by surface-coatings [12,38,49]. Although the closure of scratch wounds *in vitro* was maintained, the addition of ASC conditioned medium, unexpectedly, reduced the rate of wound healing. Likely, extracts had inactivated part of the bioactive molecules in the conditioned medium, e.g., by binding and steric hindrance or by competition of Mg^{2+} for Zn^{2+} in e.g., matrix metalloproteinases, which require Zn^{2+} for enzymatic activity. Moreover, their differentiation capacity to adipocytes, osteoblasts, and, more relevant to arterial repair, SMC is reported to be unaltered upon exposure to extracts from surface-coated materials [33,50]. No data exist in the literature on changes of differentiation of ASC to vascular cell types under the influence of Mg compounds, unfortunately. The high expression of extracellular matrix genes COL4A1 and FN1 that we observed is particularly relevant for fast arterial repair because these genes encode essential constituents of the basal membrane. Basal membrane deposition is essential for the re-endothelialization of arterial lesions, especially after placing of stents.

Nevertheless, the surface-coatings require further improvement because released components were cytotoxic to endothelial cells and also compromised pre-established vascular networks *in vitro*. However, our experiments were all performed under static conditions, which might be harsher compared to intra-arterial conditions after stenting. Then, the high flow rate on the luminal side and the interstitial flow between stent in the arterial wall, probably quickly dispose of extracts. Currently, *ex vivo* and *in vivo* experiments are in progress to investigate this presumption.

The combination of biomaterials as scaffolds to successfully deliver ASCs [51–53] is generally done in three-dimensional scaffolds. Arterial

repair, however, requires no more than the 'two-dimensional' delivery of ASC to the plane of the lesion to accelerate and stimulate the local response of repair by co-helper cells like endothelium cells.

Destruction of pre-established networks of ASC and HUVEC showed that endothelial cells are sensitive to higher Mg^{2+} concentrations, which indicates that once the degradation of the material is occurring, the recovery of the tissue may be delayed until the total elimination of the implant. It is essential to highlight that all these experiments were carried out under static conditions, which differ in the real application in which the implants will be continuously exposed to the blood flow where the Mg will be mobilized, avoiding its accumulation. *In vivo*, obviously, the bloodstream will carry away most of the corrosion products that, in our harsh static conditions, negatively impacted endothelial cells and smooth muscle cells. Alternatively, damage to the endothelial tissue due to the material can be reduced by the addition of a polymeric coating or an organic compound between the tissue-material interface to mitigate this effect. However, these experiments must be verified under *in vivo* conditions since, according to several studies, one of the limitations of the evaluation of Mg as implant is that the *in vitro* models are not precise or representative of predicting what may happen *in vivo* [54–56]. However, the somewhat 'harsh' *in vitro* settings of our experiments likely exaggerate *in vivo* conditions. Thus, animal experiments to take the material to the next level of development are warranted.

5. Conclusions

In this study, we established a platform of surface-coated Mg loaded with ASC and investigated its bioactivity in detail as a prelude to the development of novel stenting modalities to treat arterial lesions. The results show that surface-coating impact the survival of vascular cells, but support the therapeutic capacity of adhered repair cells. In terms of the composition, coatings mainly of magnesium oxide and magnesium hydroxide, these components are not harmful to the body since Mg is an essential element for the body. Our study showed that HUVEC and SMCs are more sensitive to changes of Mg. Evaluation *in vitro* has some limitations in the prediction of the performance of the materials *in vivo*; for instance, the volume ratio and the static condition of the experiments differ with the application. This *in vitro* setup is an exaggeration of the system; after an *in vivo* evaluation, it is expected a better response from the cells since the hydrogen and the degradation product of Mg can be transported and diffused by the blood flow.
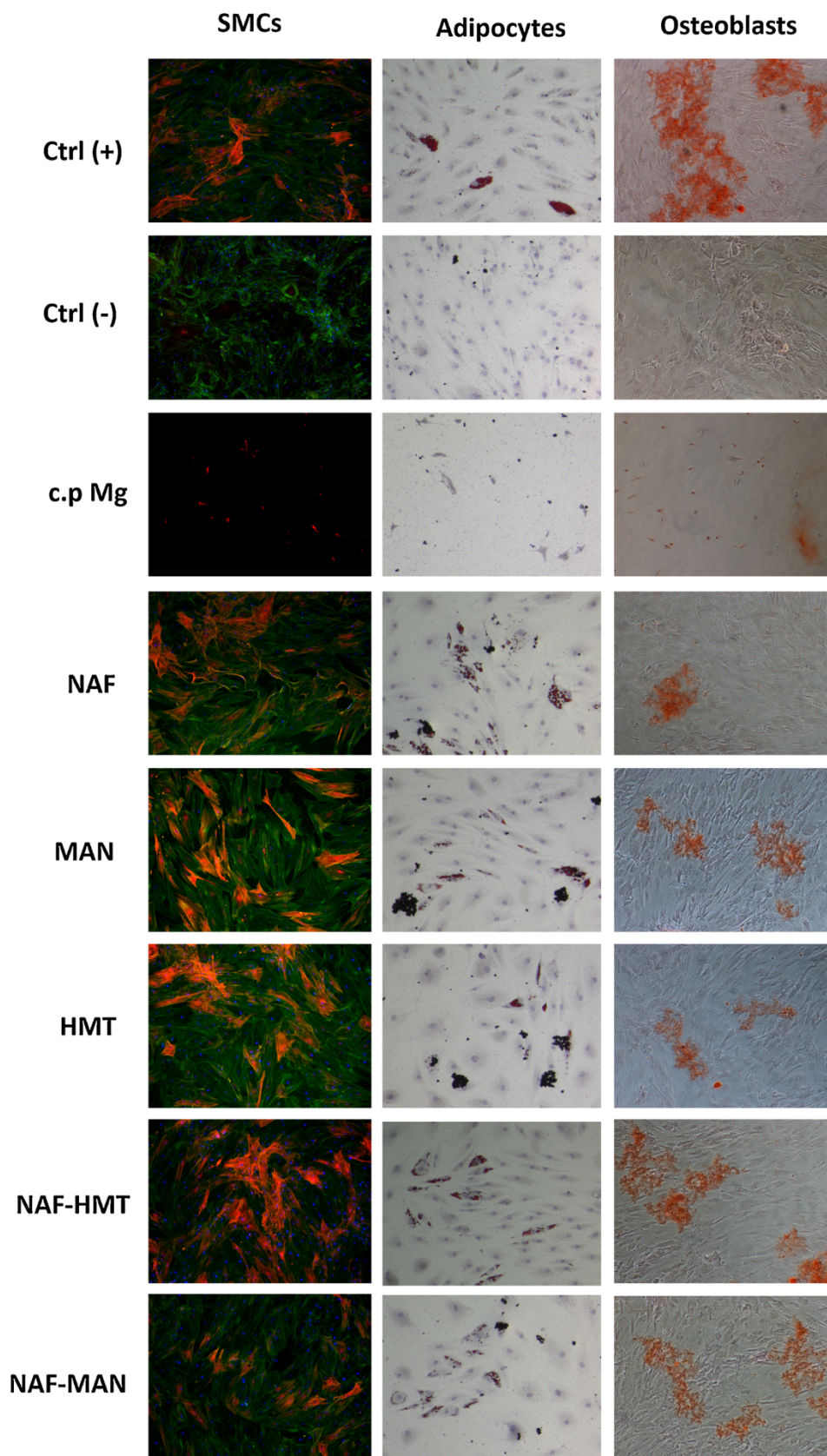
Fig. 6. Differentiation of ASC is not affected by extracts from surface-coated materials. ASCs were treated with extracts obtained by overnight incubation in culture medium of the surface-coated materials (indicated to the left) and c.p Mg as control and subjected to differential to smooth muscle cells (Green: phalloidin, red: SM22α, blue: DAPI), adipocytes (oil red O) and osteoblast (alizarin red). Differentiation was for 14 days for SMC, adipocytes and osteoblasts.
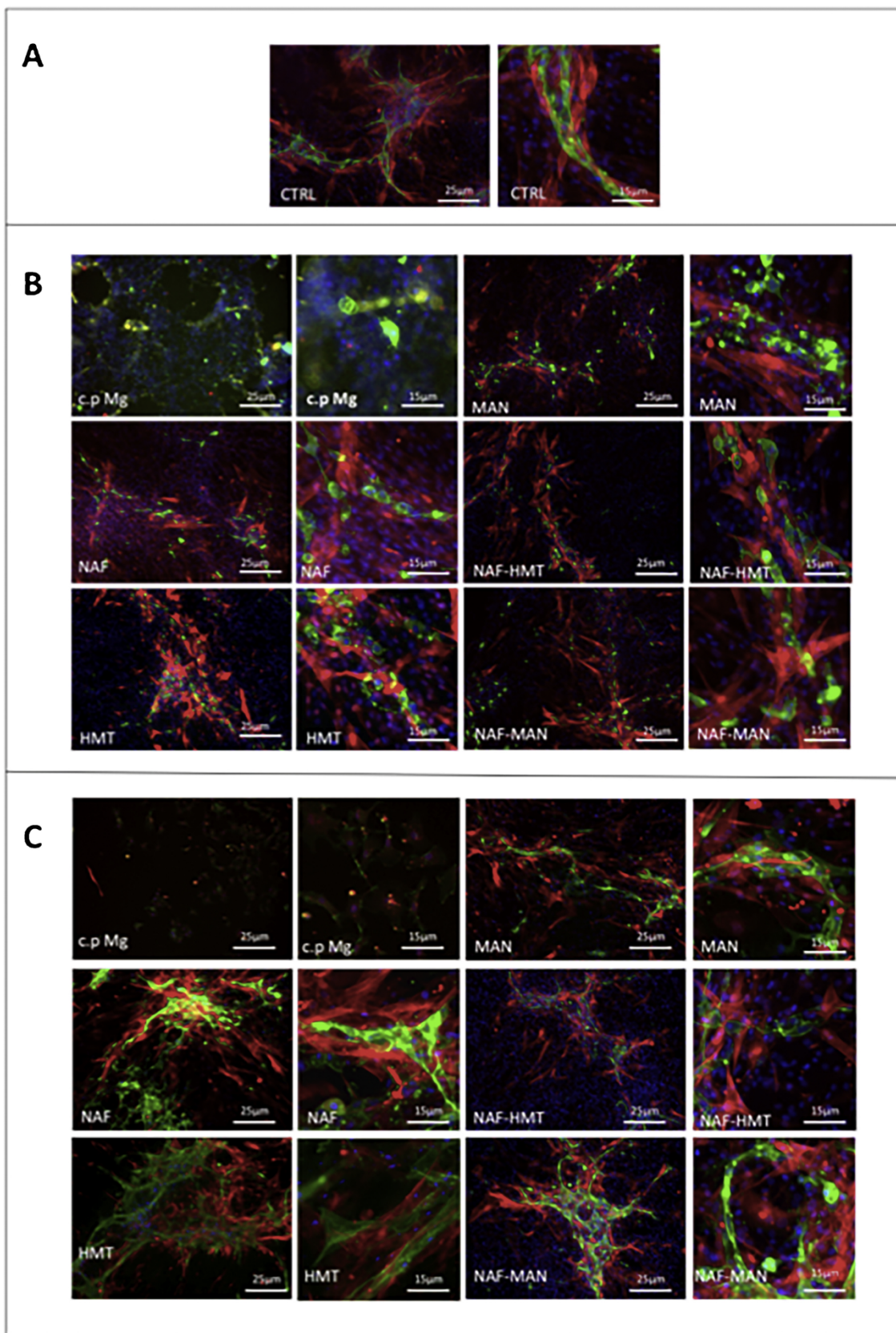
Fig. 7. Influence of materials' extracts on ASCs' capacity to support vasculogenesis *in vitro*. Panel A) Plain medium controls (CTRL) **Panel B)** Confluent monolayers of ASCs were treated with extracts obtained by incubation in culture medium of resp. NAF, HMT, MAN, NAF-HMT and NAF-MAN surface coatings and c.p Mg and their capacity was assessed to support formation of vascular-like structures by HUVECs (seeded on the ASCs and incubation for seven days. **Panel C)** HUVECs were seeded on top of confluent monolayers of ASCs and vascular-like structures allowed to form for seven days. Fluoromicrographs were recorded after overnight treatment with extracts obtained by incubation in culture medium of resp. NAF, HMT, MAN, NAF-HMT and NAF-MAN surface coatings and c.p Mg. ASCs (Red: SM22α, blue: DAPI) and HUVECs (Green: CD31, blue: DAPI).
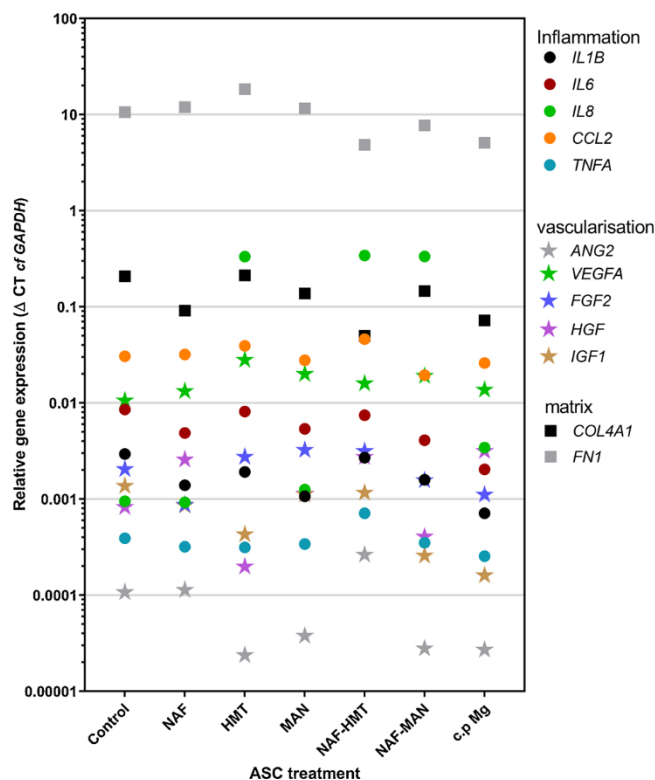
Fig. 8. Gene expression analyses of ASC after exposure to surface-coated materials' l extracts. Expression of genes is expressed as fold-difference (ΔC_T) to expression of the reference gene *GAPDH*. Extracts obtained after overnight incubation in medium of resp. NAF, HMT, MAN, NAF-HMT and NAF-MAN surface coatings and c.p Mg controls were used to treat ASCs (n = 3 donors) overnight. Expression of genes representing inflammatory activation (*IL1B, IL6, IL8, CCL2* and *TNFA*), angiogenesis and regeneration (*ANG2, VEGFA, FGF2, HGF* and *IGF1*) and extracellular matrix genes (*FN1* and *COL4A1*) were assessed by RT-qPCR. Data plotted are from three donors with technical triplicate.

CRediT authorship contribution statement

Monica Echeverry-Rendon: Conceptualization, Data curation, Formal analysis, Investigation, Methodology, Writing - original draft, Writing - review & editing. **Felix Echeverria:** Conceptualization, Supervision, Writing - review & editing. **Martin C. Harmsen:** Conceptualization, Data curation, Formal analysis, Funding acquisition, Investigation, Supervision, Writing - review & editing.

Declaration of competing interest

The authors declare that they have no known competing financial interests or personal relationships that could have appeared to influence the work reported in this paper.

Acknowledgements

Appendix A. Supplementary data

Supplementary material related to this article can be found, in the online version, at doi:https://doi.org/10.1016/j.colsurfb.2020.111153.

References

[1] WHO World Health Statistics 2014, n.d.
[2] E.G. Lakatta, D. Levy, Arterial and cardiac aging: major shareholders in cardiovascular disease enterprises: part I: aging arteries: a "set up" for vascular disease, Circulation 107 (2003) 139–146.
[3] E.G. Lakatta, D. Levy, Arterial and cardiac aging: major shareholders in cardiovascular disease enterprises: part II: the aging heart in health: links to heart disease, Circulation 107 (2003) 346–354.
[4] D. Roy, G. Milot, J. Raymond, Endovascular treatment of unruptured aneurysms, Stroke 32 (2001) 1998–2004.
[5] R. Ross, The pathogenesis of atherosclerosis—an update, N. Engl. J. Med. 314 (1986) 488–500.
[6] S. Ramcharitar, P.W. Serruys, Fully biodegradable coronary stents : progress to date, Am. J. Cardiovasc. Drugs 8 (2008) 305–314 http://www.ncbi.nlm.nih.gov/pubmed/18828642.
[7] P. Radke, Outcome after treatment of coronary in-stent restenosis results from a systematic review using meta-analysis techniques, Eur. Heart J. 24 (2003) 266–273, https://doi.org/10.1016/S0195-668X(02)00202-6.
[8] K.E. Robertson, R.A. McDonald, K.G. Oldroyd, S.A. Nicklin, A.H. Baker, Prevention of coronary in-stent restenosis and vein graft failure: does vascular gene therapy have a role? Pharmacol. Ther. 136 (2012) 23–34, https://doi.org/10.1016/j.pharmthera.2012.07.002.
[9] S. Morlacchi, F. Migliavacca, Modeling stented coronary arteries: where we are, where to go, Ann. Biomed. Eng. 41 (2013) 1428–1444, https://doi.org/10.1007/s10439-012-0681-6.
[10] I. Akin, H. Schneider, H. Ince, S. Kische, T.C. Rehders, T. Chatterjee, C. a Nienaber, Second- and third-generation drug-eluting coronary stents: progress and safety, Herz 36 (2011) 190–196, https://doi.org/10.1007/s00059-011-3458-z.
[11] R.A. Partida, R.W. Yeh, Contemporary drug-eluting stent platforms: design, safety, and clinical efficacy, Interv. Cardiol. Clin. 5 (2016) 331–347.
[12] S. Pant, G. Limbert, N.P. Curzen, N.W. Bressloff, Multiobjective design optimisation of coronary stents, Biomaterials 32 (2011) 7755–7773, https://doi.org/10.1016/j.biomaterials.2011.07.059.
[13] J. Foerst, M. Vorpahl, T. Koehler, K. Tiroch, R. Wessely, Evolution of coronary stents: from bare-metal stents to fully biodegradable, drug-eluting stents, Comb. Prod. Ther. 3 (2013) 9–24, https://doi.org/10.1007/s13556-013-0005-7.
[14] M.-C. Chen, C.-T. Liu, H.-W. Tsai, W.-Y. Lai, Y. Chang, H.-W. Sung, Mechanical properties, drug eluting characteristics and in vivo performance of a genipin-crosslinked chitosan polymeric stent, Biomaterials 30 (2009) 5560–5571.
[15] C. Di Mario, H.U.W. Griffiths, O. Goktekin, N. Peeters, J.A.N. Verbist, M. Bosiers, K. Deloose, B. Heublein, R. Rohde, V. Kasese, et al., Drug-eluting bioabsorbable magnesium stent, J. Interv. Cardiol. 17 (2004) 391–395.
[16] B. O'Brien, W. Carroll, The evolution of cardiovascular stent materials and surfaces in response to clinical drivers: a review, Acta Biomater. 5 (2009) 945–958, https://doi.org/10.1016/j.actbio.2008.11.012.
[17] J. Jagur-Grodzinski, Polymers for tissue engineering, medical devices, and regenerative medicine. Concise general review of recent studies, Polym. Adv. Technol. 17 (2006) 395–418.
[18] L.P. Gough, Element Concentrations Toxic to Plants, Animals, and Man, (1979).
[19] M. Shechter, A. Shechter, Magnesium in Human Health and Disease, (2013), https://doi.org/10.1007/978-1-62703-044-1.
[20] J. Kuhlmann, I. Bartsch, E. Willbold, S. Schuchardt, O. Holz, N. Hort, D. Höche, W.R. Heineman, F. Witte, Fast escape of hydrogen from gas cavities around corroding magnesium implants, Acta Biomater. 9 (2013) 8714–8721.
[21] G.S. Frankel, A. Samaniego, N. Birbilis, Evolution of hydrogen at dissolving magnesium surfaces, Corros. Sci. 70 (2013) 104–111.
[22] A. Abdal-hay, M. Dewidar, J. Lim, J. Kyoo, Enhanced biocorrosion resistance of surface modi fi ed magnesium alloys using inorganic / organic composite layer for biomedical applications, Ceram. Int. 40 (2014) 2237–2247.
[23] W. Jin, G. Wu, H. Feng, W. Wang, X. Zhang, P.K. Chu, Improvement of corrosion resistance and biocompatibility of rare-earth WE43 magnesium alloy by neodymium self-ion implantation, Corros. Sci. 94 (2015) 142–155, https://doi.org/10.1016/j.corsci.2015.01.049.
[24] C. Lorenz, J.G. Brunner, P. Kollmannsberger, L. Jaafar, B. Fabry, S. Virtanen, Effect of surface pre-treatments on biocompatibility of magnesium, Acta Biomater. 5 (2009) 2783–2789, https://doi.org/10.1016/j.actbio.2009.04.018.
[25] T.S.N. Sankara Narayanan, I.S. Park, M.H. Lee, Strategies to improve the corrosion resistance of microarc oxidation (MAO) coated magnesium alloys for degradable implants: prospects and challenges, Prog. Mater. Sci. 60 (2014) 1–71, https://doi.org/10.1016/j.pmatsci.2013.08.002.
[26] G.B. Darband, M. Aliofkhazraei, P. Hamghalam, N. Valizade, Plasma electrolytic oxidation of magnesium and its alloys: mechanism, properties and applications, J. Magnes. Alloy. 5 (2017) 74–132.
[27] B.L. Jiang, Y.F. Ge, Micro-arc oxidation (MAO) to improve the corrosion resistance of magnesium (Mg) alloys, Corros. Prev. Magnes. Alloy, Elsevier, 2013, pp. 163–196.
[28] Y. Jang, Z. Tan, C. Jurey, B. Collins, A. Badve, Z. Dong, C. Park, C.S. Kim, J. Sankar, Y. Yun, Systematic understanding of corrosion behavior of plasma electrolytic oxidation treated AZ31 magnesium alloy using a mouse model of subcutaneous implant, Mater. Sci. Eng. C (2014), https://doi.org/10.1016/j.msec.2014.08.052.
[29] Y. Gao, A. Yerokhin, A. Matthews, Applied surface science effect of current mode on PEO treatment of magnesium in Ca- and P-containing electrolyte and resulting coatings, Appl. Surf. Sci. 316 (2014) 558–567, https://doi.org/10.1016/j.apsusc.2014.08.035.

[30] M. Echeverry-Rendon, V. Duque, D. Quintero, M.C. Harmsen, F. Echeverria, Novel coatings obtained by plasma electrolytic oxidation to improve the corrosion resistance of magnesium-based biodegradable implants, Surf. Coatings Technol. 354 (2018) 28–37.

[31] W.R. Zhou, Y.F. Zheng, M. a Leeflang, J. Zhou, Mechanical property, biocorrosion and in vitro biocompatibility evaluations of Mg-Li-(Al)-(RE) alloys for future cardiovascular stent application, Acta Biomater. 9 (2013) 8488–8498, https://doi.org/10.1016/j.actbio.2013.01.032.

[32] L. Choudhary, R.K.S. Raman, Magnesium alloys as body implants: fracture mechanism under dynamic and static loadings in a physiological environment, Acta Biomater. 8 (2012) 916–923, https://doi.org/10.1016/j.actbio.2011.10.031.

[33] M. Parvizi, A.H. Petersen, C. van Spreuwel-Goossens, S. Kluijtmans, M.C. Harmsen, Perivascular scaffolds loaded with adipose tissue-derived stromal cells attenuate development and progression of abdominal aortic aneurysm in rats, J. Biomed. Mater. Res. Part A (2018).

[34] G. Bassi, L. Pacelli, R. Carusone, J. Zanoncello, M. Krampera, Adipose-derived stromal cells (ASCs), Transfus. Apher. Sci. 47 (2012) 193–198.

[35] M. Echeverry-Rendon, J.P. Allain, S.M. Robledo, F. Echeverria, M.C. Harmsen, Coatings for biodegradable magnesium-based supports for therapy of vascular disease: a general view, Mater. Sci. Eng. C. Mater. Biol. Appl. 102 (2019) 150.

[36] M. Echeverry-Rendon, V. Duque, D. Quintero, S.M. Robledo, M.C. Harmsen, F. Echeverria, Improved corrosion resistance of commercially pure magnesium after its modification by plasma electrolytic oxidation with organic additives, J. Biomater. Appl. 33 (2018) 725–740.

[37] G. Hajmousa, E. Przybyt, F. Pfister, G.A. Paredes-Juarez, K. Moganti, S. Busch, J. Kuipers, I. Klaassen, M.J.A. van Luyn, G. Krenning, et al., Human adipose tissue-derived stromal cells act as functional pericytes in mice and suppress high-glucose-induced proinflammatory activation of bovine retinal endothelial cells, Diabetologia 61 (2018) 2371–2385.

[38] V. Terlizzi, M. Kolibabka, J.K. Burgess, H.P. Hammes, M.C. Harmsen, The pericytic phenotype of adipose tissue-derived stromal cells Is promoted by NOTCH2, Stem Cells 36 (2018) 240–251.

[39] J.P. Allain, M. Echeverry-Rendón, Surface Treatment of Metallic Biomaterials in Contact With Blood to Enhance Hemocompatibility, (2017), https://doi.org/10.1016/B978-0-08-100497-5.00008-2.

[40] M. Yeganeh, N. Mohammadi, Superhydrophobic surface of Mg alloys: a review, J. Magnes. Alloy 6 (2018) 59–70.

[41] D. Khatayevich, M. Gungormus, H. Yazici, C. So, S. Cetinel, H. Ma, A. Jen, C. Tamerler, M. Sarikaya, Biofunctionalization of materials for implants using engineered peptides, Acta Biomater. 6 (2010) 4634–4641, https://doi.org/10.1016/j.actbio.2010.06.004.

[42] P. Tian, X. Liu, Surface modification of biodegradable magnesium and its alloys for biomedical applications, Regen. Biomater. 2 (2015) 135–151.

[43] A.F. Anvari-Yazdi, K. Tahermanesh, S.M.M. Hadavi, T. Talaei-Khozani, M. Razmkhah, S.M. Abed, M.S. Mohtasebi, Cytotoxicity assessment of adipose-derived mesenchymal stem cells on synthesized biodegradable Mg-Zn-Ca alloys, Mater. Sci. Eng. C 69 (2016) 584–597.

[44] B.J.C. Luthringer, R. Willumeit-Römer, Effects of magnesium degradation products on mesenchymal stem cell fate and osteoblastogenesis, Gene 575 (2016) 9–20.

[45] Y. Yun, Z. Dong, D. Yang, M.J. Schulz, V.N. Shanov, S. Yarmolenko, Z. Xu, P. Kumta, C. Sfeir, Biodegradable Mg corrosion and osteoblast cell culture studies, Mater. Sci. Eng. C 29 (2009) 1814–1821.

[46] J. Zhang, S. Hiromoto, T. Yamazaki, H. Huang, G. Jia, H. Li, G. Yuan, Macrophage phagocytosis of biomedical Mg alloy degradation products prepared by electrochemical method, Mater. Sci. Eng. C 75 (2017) 1178–1183.

[47] I. Roth, S. Schumacher, T. Basler, K. Baumert, J.-M. Seitz, F. Evertz, P.P. Müller, W. Bäumer, M. Kietzmann, Magnesium corrosion particles do not interfere with the immune function of primary human and murine macrophages, Prog. Biomater. 4 (2015) 21–30.

[48] F. Alvarez, R.M.L. Puerto, B. Pérez-Maceda, C.A. Grillo, M.F.L. de Mele, Time-lapse evaluation of interactions between biodegradable Mg particles and cells, Microsc. Microanal. 22 (2016) 1–12.

[49] G. Hajmousa, A.A. Elorza, V.J.M. Nies, E.L. Jensen, R.A. Nagy, M.C. Harmsen, Hyperglycemia induces bioenergetic changes in adipose-derived stromal cells while their pericytic function is retained, Stem Cells Dev. 25 (2016) 1444–1453.

[50] M. Parvizi, L.A.M. Bolhuis-Versteeg, A.A. Poot, M.C. Harmsen, Efficient generation of smooth muscle cells from adipose-derived stromal cells by 3D mechanical stimulation can substitute the use of growth factors in vascular tissue engineering, Biotechnol. J. 11 (2016) 932–944.

[51] C. Nie, D. Yang, S.F. Morris, Local delivery of adipose-derived stem cells via acellular dermal matrix as a scaffold: a new promising strategy to accelerate wound healing, Med. Hypotheses 72 (2009) 679–682.

[52] A.M. Altman, Y. Yan, N. Matthias, X. Bai, C. Rios, A.B. Mathur, Y.-H. Song, E.U. Alt, IFATS collection: human adipose-derived stem cells seeded on a silk fibroin-chitosan scaffold enhance wound repair in a murine soft tissue injury model, Stem Cells 27 (2009) 250–258.

[53] H.K. Cheung, T.T.Y. Han, D.M. Marecak, J.F. Watkins, B.G. Amsden, L.E. Flynn, Composite hydrogel scaffolds incorporating decellularized adipose tissue for soft tissue engineering with adipose-derived stem cells, Biomaterials 35 (2014) 1914–1923.

[54] P.K. Bowen, A. Drelich, J. Drelich, J. Goldman, Rates of in vivo (arterial) and in vitro biocorrosion for pure magnesium, J. Biomed. Mater. Res. Part A 103 (2015) 341–349.

[55] N.I.Z. Abidin, B. Rolfe, H. Owen, J. Malisano, D. Martin, J. Hofstetter, P.J. Uggowitzer, A. Atrens, The in vivo and in vitro corrosion of high-purity magnesium and magnesium alloys WZ21 and AZ91, Corros. Sci. 75 (2013) 354–366.

[56] P.K. Bowen, J. Drelich, J. Goldman, A new in vitro-in vivo correlation for bioabsorbable magnesium stents from mechanical behavior, Mater. Sci. Eng. C. Mater. Biol. Appl. 33 (2013) 5064–5070, https://doi.org/10.1016/j.msec.2013.08.042.